THE ASTROPHYSICAL JOURNAL, 462:L43–L47, 1996 May 1

ATOMIC OXYGEN IN MOLECULAR CLOUDS? HIGH-RESOLUTION SPECTROSCOPY OF THE [O I] 63 MICRON LINE TOWARD DR 21

A. POGLITSCH, F. HERRMANN, R. GENZEL, S. C. MADDEN,[1] T. NIKOLA, AND R. TIMMERMANN
Max-Planck-Institut für Extraterrestrische Physik, D-85740 Garching, Germany

N. GEIS
Department of Physics, University of California, Berkeley, CA 94720

AND

G. J. STACEY
Department of Astronomy, Cornell University, Ithaca, NY 14853
Received 1995 December 11; accepted 1996 February 21

ABSTRACT

We report the first high-resolution spectra of the [O I] 63 μm fine-structure line toward DR 21. The observations were made from NASA's Kuiper Airborne Observatory using the MPE/UCB imaging spectrometer FIFI. The spectra show a pronounced dip, which may be due to absorption by a foreground molecular cloud, seen against the broad [O I] emission from DR 21. In this case we derive a column density of cold, atomic oxygen of $\gtrsim 5 \times 10^{18}$ cm^{-2}, corresponding to a relative abundance of atomic oxygen of [O]/[H] $\gtrsim 6 \times 10^{-4}$. Therefore, most of the gas-phase oxygen in this cloud would be in atomic form. This result is in contrast to predictions by common chemistry models for a steady state cloud and may support models which predict a high abundance of atomic oxygen in dark cores of molecular clouds.

Subject headings: infrared: ISM: lines and bands — ISM: abundances

1. INTRODUCTION

The nature of the repository of oxygen in the dark, quiescent component of the interstellar medium is one of the outstanding open questions in interstellar chemistry. Oxygen is the third-most abundant element in the universe, and its depletion onto dust grains is believed to be small ($\delta \lesssim 25\%$; van Dishoeck et al. 1993; Greenberg 1991). Most of the interstellar oxygen, therefore, should reside in the gas phase of the ISM where the principal species are CO, O_2, O, H_2O, and OH. Out of these only, CO has been observed in appreciable amounts, but can account only for ~10% of the total oxygen abundance, and the abundance of gas-phase H_2O is significantly lower yet (Plambeck & Wright 1987; Jacq et al. 1988, 1990; Knacke & Larson 1991; Cernicharo et al. 1994; Tauber et al. 1996; Zmuidzinas et al. 1995). Chemical models predict that, at least in steady state, the majority of the oxygen should be found in the form of O_2 and other molecules (Herbst & Leung 1989; Millar et al. 1991) unless cosmic-ray–induced photodissociation plays a major role (Gredel et al. 1989; Sternberg & Dalgarno 1995). Searches for $^{16}O^{18}O$ in a number of dark clouds have been unsuccessful so far and pose upper limits on the O_2/CO abundance ratio that are of the order 20% (Goldsmith et al. 1985; Liszt & Vanden Bout 1985; Fuente et al. 1993). A recent, direct search for O_2 in a redshifted, single molecular cloud has even found an upper limit of ~1% for this ratio (Combes & Wiklind 1995).

Therefore, we began a search for atomic oxygen in molecular clouds using the [O I] 63 μm fine-structure line. With a 228 K upper level for the 63 μm ground-state transition, only an absorption experiment seemed promising for a quantitative measurement in cold gas, and DR 21 a well-suited source for this. DR 21 shows strong [O I] 63 μm emission associated with the H II region/outflow (Lane et al. 1990); for instrumental reasons this fairly broad emission line makes a better background source than continuum emission for the observation of absorption by foreground material.

The molecular gas toward DR 21 contains two components, one at $v_{LSR} \approx -3$ km s^{-1} which is associated with the H II region/cloud core, and one at $v_{LSR} \approx 8$ km s^{-1} which seems to be an extension of the W75 N molecular ridge. While the −3 km s^{-1} component contains fairly warm gas and is closely related to the DR 21 star-forming region (Jaffe et al. 1989), there is no such indication for the +8 km s^{-1} component, which is seen only in low-J CO line emission (Dickel, Dickel, & Wilson 1978; Fischer et al. 1985; Garden et al. 1991) and in H_2CO absorption against the 6 cm continuum from the H II region (Bieging, Wilson, & Downes 1982; Dickel et al. 1983). It is also seen as a self-absorption feature in the CO(2 → 1) spectra but not in the CO(7 → 6) spectra (Jaffe et al. 1989). It is therefore assumed that this component represents detached, cold foreground gas, which makes it a good candidate for an absorption experiment to detect cold atomic oxygen in a molecular cloud.

2. OBSERVATIONS

The observations of the $^3P_1 \rightarrow {}^3P_2$ [O I] 63.1837 μm line were carried out with the MPE/UCB Far-infrared Imaging Fabry-Pérot Interferometer (Poglitsch et al. 1991; Stacey et al. 1992) during three flights with NASA's Kuiper Airborne Observatory (KAO) from Hickam Airforce Base, HI, on 1992 August 19 and 23 and 1994 May 24. The oscillating secondary mirror of the telescope was chopped at 21 Hz with a throw of ~5′ in SE-NW direction in 1992 and ~7.′5 in N-S direction in 1994. Beams were switched in ~1 minute intervals by nodding the telescope. The geometrical pixel size of our 5 × 5 pixel detector array was 20″ × 20″; the beam size was ~22″ FWHM

[1] Present address: NASA Ames Research Center, Moffett Field, CA 94035.

with a corresponding beam solid angle of 1.3×10^{-8} sr. The image rotator was set to a position angle of 45° for maximum coverage in E-W direction.

Data were taken at three different spectral resolutions: 30 km s^{-1}, 20 km s^{-1}, and 7 km s^{-1}. For the 30 km s^{-1} resolution spectra taken in 1992 the scan width was 300 km s^{-1}, centered at $v_{LSR} \approx 0$ km s^{-1}, and the total integration time was 42 minutes. The center position was R.A. = $20^h37^m15\overset{s}{.}3$, decl. = 42°08′45″ (1950). For the 20 km s^{-1} resolution spectra taken in 1992, the scan width was 140 km s^{-1}, centered at $v_{LSR} \approx 0$ km s^{-1}, and the total integration time was 20 minutes. The center position was R.A. = $20^h37^m18\overset{s}{.}0$, decl. = 42°09′05″ (1950). Observations at 7 km s^{-1} resolution were carried out in 1992 and 1994; in both cases the scan width was 55 km s^{-1}, but the scan center was at $v_{LSR} \approx 0$ km s^{-1} for the data taken in 1992, whereas in 1994 the scan center was shifted to $v_{LSR} \approx 10$ km s^{-1}. The integration time in 1992 was 37 minutes; in 1994 we obtained only 13 minutes of useful observing time because of telescope problems. The center positions were R.A. = $20^h37^m15\overset{s}{.}3$, decl. = 42°09′05″ (1950) and R.A. = $20^h37^m16\overset{s}{.}9$, decl. = 2°08′50″ (1950), respectively.

The Doppler shift along the line of sight toward DR 21 was −17.6 km s^{-1} for the 1992 observations and −32.7 km s^{-1} for the 1994 observations. This difference of 15 km s^{-1} was useful for discerning astronomical lines from telluric features. Wavelength was calibrated with two ammonia lines ($\lambda = 63.2054$ μm and $\lambda = 63.1255$ μm) in a gas absorption cell. For the observations made at 7 km s^{-1} resolution, the error in the velocity scale is estimated to be ±2 km s^{-1}. Flat fielding was done with internal calibration sources. For absolute intensity calibration we used the continuum emission from Sgr B2, assuming a flux of 10^4 Jy at 63 μm (Gatley et al. 1978), and the continuum emission from Jupiter, which was assumed to emit like a 130 K blackbody (Hildebrand et al. 1985). The errors in absolute intensity for line detection depend on the resolution; we estimate them to be ≤30% at 30 km s^{-1} and 20 km s^{-1}, and ≤50% at 7 km s^{-1}.

3. RESULTS

The spectra obtained on individual pixels are shown in Figure 1 for the three spectral resolutions observed in 1992 (Herrmann 1993). East is in the upper left corner of the detector array, west in the lower right. Please note that the pointing was different for each observation. The prominent peak in continuum emission associated with the H II region (Lane et al. 1990) appears on different pixels in the three observations and may be used for orientation. The apparent line-to-continuum ratio also varies with spectral resolution; this is an instrumental effect in that the resolution bandwidth relevant for line detection and the detection bandwidth for continuum radiation differ by a factor that increases with spectral resolution. This "leakage" factor is $f_{leak} \approx 2$ at 30 km s^{-1}, $f_{leak} \approx 3$ at 20 km s^{-1}, and $f_{leak} \approx 8.5$ at 7 km s^{-1} resolution for continuum detection over line detection; for an "ideal" instrument it would be unity.

Lane et al. (1990) found the peak in integrated [O I] line intensity offset by ∼1′ to the east (left and up on the detector array) from the continuum peak. Our lower resolution spectra (Figs. 1*a*–1*b*) show that this is partly an effect of line width that is greater toward their [O I] peak position than toward the continuum peak/H II region. This indicates a close relationship of the [O I] peak with the eastern lobe of the outflow while at

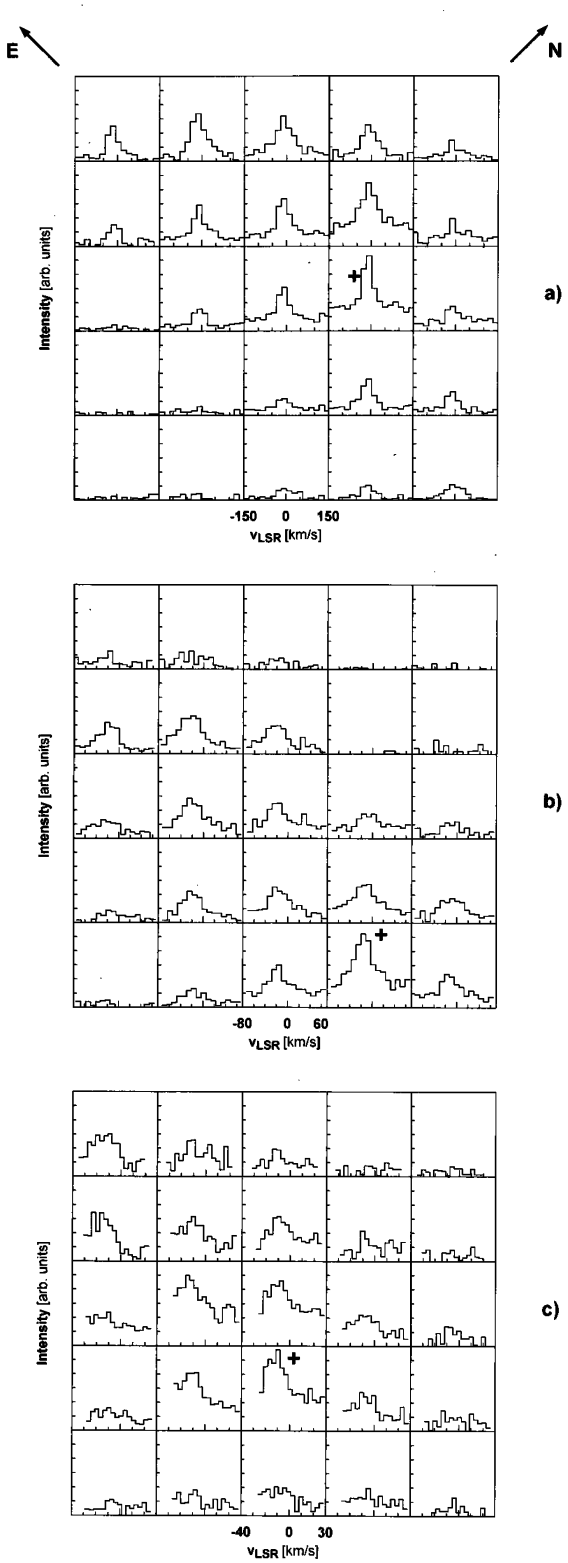

FIG. 1.—[O I] 63 μm spectra toward DR 21 at three different spectral resolutions (1992 data set; Herrmann 1993). (*a*) 30 km s^{-1}; (*b*) 20 km s^{-1}; (*c*) 7 km s^{-1}. Note that the pointing is different in each case; the radio continuum centroid position is indicated by the crosses. Intensity values start at zero for all pixels.

the same time the excitation mechanism for the FIR fine structure line emission is dominated by UV heating (Lane et al. 1990).

The high-resolution spectra (Fig. 1*c*) reveal a new feature: a dip in the spectrum at $v_{LSR} \sim 9$ km s^{-1}, which seems to be present on all pixels that show significant [O I] emission, but most prominent toward the position of the [O I] peak in the map of Lane et al. (1990), which is in the upper left corner of the array. We therefore selected this position for a quantitative analysis. Furthermore, the continuum level is fairly low there as seen from the spectra at all resolutions. A low continuum level is advantageous since the limited scan width at the highest resolution does not allow a very accurate determination of the baseline, and a correct prediction of the continuum level from the low-resolution observations is hampered by the very large "leakage" factor, i.e., enhancement of continuum detection over line detection by contributions from adjacent, unsuppressed Fabry-Pérot orders, at high spectral resolutions. Separation into line emission and continuum emission, however, is essential in a quantitative detection of a potential absorption line with our instrument because the apparent optical depth is also reduced by the leakage factor when observed against a continuum source versus a narrowband source. A low continuum level makes this procedure less critical.

The co-averaged spectra of the two or three pixels closest to the [O I] peak position are shown in Figure 2*a* for the three different spectral resolutions. The dip at $v_{LSR} \sim 9$ km s^{-1} is very prominent in the 7 km s^{-1} resolution spectrum; there is also an indication of it in the 20 km s^{-1} spectrum and still some asymmetry in the 30 km s^{-1} spectrum. Figure 2*b* shows a less binned version of the high-resolution spectrum together with the spectrum taken in 1994, which is also the average of 2 pixels toward the [O I] peak position. Due to the short integration time, the signal-to-noise ratio is lower for the second data set, but the agreement is still good, and the extension of the scan to greater positive velocities makes the dip even more significant.

If we assume for now that the observed spectrum represents broad emission from the outflow with a narrow absorption line from colder foreground gas then we may model the source spectrum by a Gaussian emission line plus continuum radiation. The line and continuum are then both attenuated according to a Gaussian distribution of optical depth in the foreground gas, but not in identical ways due to the continuum "leakage" as mentioned above:

$$I(v) = I_0 \exp\left[-\left(\frac{v - v_I}{\sigma_I}\right)^2\right] \exp\left[-\tau(v)\right] + C_0\left\{1 - \frac{1 - \exp\left[-\tau(v)\right]}{f_{\text{leak}}}\right\}, \quad (1)$$

where I_0 denotes the peak line intensity, C_0 is the total detected continuum, f_{leak} accounts for "leakage" from unsuppressed adjacent Fabry-Pérot orders, and the optical depth τ as a function of velocity is given by

$$\tau(v) = \tau_0 \exp\left[-\left(\frac{v - v_\tau}{\sigma_\tau}\right)^2\right]. \quad (2)$$

This spectrum is then convolved with the instrument function $F(v)$, which can be approximated by a Lorentzian profile. The

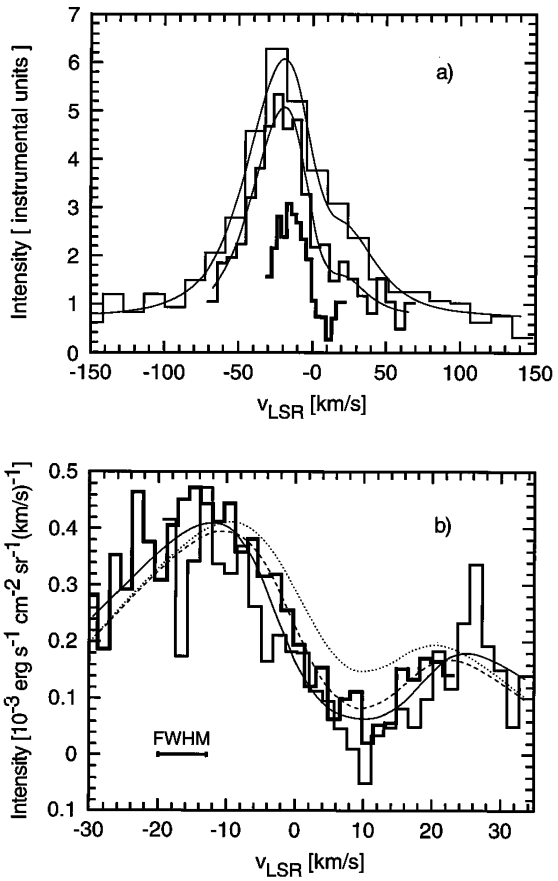

FIG. 2.—[O I] 63 μm spectra toward the DR 21 [O I] emission peak at three different spectral resolutions. (*a*) *Thin line*, 30 km s^{-1}; *solid line*, 20 km s^{-1}; *heavy line*, 7 km s^{-1} (1992). Also shown are the fits at 30 km s^{-1} and 20 km s^{-1} as thin lines; calculated with $\tau_0 = 5.9$. (*b*) Spectra at 7 km s^{-1} resolution. *Heavy line*, 1992 data; *solid line*, 1994 data. The thin, continuous line represents the fitted spectrum with $\tau_0 = 5.9$; the thin, dashed line and the thin, dotted line represent fits with $\tau_0 = 2.5$ and $\tau_0 = 1.5$, respectively.

20 and 30 km s^{-1} resolution spectra from Figure 2*a* were used together with the combined 7 km s^{-1} resolution spectra from Figure 2*b* for a simultaneous least-square fit procedure where the lower resolution spectra mainly entered into the parameters of the emission, and the absorption line was mainly derived from the high-resolution spectra. The best-fit spectra, with $\tau_0 = 5.9$ and $\sigma_\tau = 7.8$ km s^{-1}, are shown as the thin lines in Figure 2*a* and as the thin continuous line in Figure 2*b*. However, since the derived peak optical depth of the absorption line is fairly high ($\tau_0 = 5.9$) one must be careful about the significance of this number, particularly because small errors in the baseline due to imbalance of the beams cannot be precluded. For comparison, the thin dashed line in Figure 2*b* represents a fit where the peak optical depth was kept fixed at $\tau_0 = 2.5$, with only a marginal decrease in the quality of the fit. We then kept all other parameters fixed and reduced the optical depth to $\tau_0 = 1.5$. In this case (thin dotted line in Fig. 2*b*) the deviation from the observed spectrum is significant, and we conclude that the peak optical depth must be $\tau_0 \gtrsim 2$.

From the optical depth of the absorption line one can derive the column density of atomic oxygen. If the absorbing gas is cold foreground material then we may assume that all oxygen

atoms are in the ground state, and the column density of oxygen is given by (Spitzer 1978)

$$N(\mathrm{O}^0) = \frac{g_l}{g_u}\frac{8\pi}{\lambda^3 A_{ul}}\int \tau(v)\,dv. \quad (3)$$

With $A_{ul} = 8.46 \times 10^{-5}$ s^{-1} (Baluja & Zeippen 1988), $\tau_0 \gtrsim 2$ and $\sigma_\tau = 7.8$ km s^{-1}, an oxygen column density of $\gtrsim 5 \times 10^{18}$ cm^{-2} is found. The column density of molecular hydrogen in the 8 km s^{-1} foreground cloud as derived from ^{13}CO observations is 4×10^{21} cm^{-2} (Dickel et al. 1978); from the ^{12}CO observations by Garden et al. (1991) we derive a column density of $\sim 3.5 \times 10^{21}$ cm^{-2}, using the conversion factor of Strong et al. (1988). Thus, the abundance of atomic oxygen is $[\mathrm{O}]/[\mathrm{H}] \gtrsim 6 \times 10^{-4}$. If we assume a solar abundance of $[\mathrm{O}]/[\mathrm{H}] = 8.5 \times 10^{-4}$ (Anders & Grevesse 1989) and a 25% depletion for the oxygen in the gas phase (van Dishoeck et al. 1993), then this means that most of the gas-phase oxygen must be in atomic form.

4. DISCUSSION

In our analysis of the spectra we have made the assumption that they represent a broad emission line and a narrow absorption line. Of course, one could create the same spectrum from two emission components at roughly -12 km s^{-1} and roughly $+24$ km s^{-1}, respectively, and there is no unambiguous way to distinguish between these cases. Indeed, the red and blue wings of the outflow extend out to ± 20 km s^{-1}. However, no other observation has shown comparably pronounced features in emission or absorption at these velocities. Therefore, the interpretation we have adopted seems plausible, even though not conclusive.

If we assume that our interpretation is justified, then the abundance of atomic oxygen is clearly much higher than predicted by most models for a steady state cloud (Herbst & Leung 1989; Langer & Graedel 1989; Gredel et al. 1989; Millar et al. 1991). On the other hand, models that take into account cosmic-ray–induced photodissociation predict that a major fraction (Gredel et al. 1989) or most of the gas phase oxygen is in atomic form (Sternberg & Dalgarno 1995). Our measurements could support the latter case, unless the cloud is in an early phase according to the time-dependent models or there is another process that keeps the oxygen in atomic form, e.g., UV penetration into the cloud. Given the relatively low H_2 column density (4×10^{21} cm^{-2}; Dickel et al. 1978) this could be a realistic possibility. There is, however, no indication of warm gas associated with the $+8$ km s^{-1} cloud or of a nearby source of UV radiation.

The question remains how unique or how general this result may be. For example, the density of the $+8$ km s^{-1} cloud ($\sim 10^4$ cm^{-3}; Dickel et al. 1983) is not very high, and it may not be a "typical" molecular cloud. Also, it is curious that we do not see a comparable absorption feature from the -3 km s^{-1} cloud associated with DR 21 itself, although it has a higher H_2 column density ($\sim 10^{22}$ cm^{-2} toward the [O I] peak position; Dickel et al. 1978; Garden et al. 1991) than the $+8$ km s^{-1} foreground cloud. There could be two reasons for this: first, most of the oxygen might be tied up in molecules due to different physical cloud parameters, and our measurements would set an upper limit of $[\mathrm{O}]/[\mathrm{H}] \sim 5 \times 10^{-5}$ to the atomic oxygen abundance; second, it could be a morphology effect. Absorption at the systemic velocity of DR 21 has been observed only against the radio continuum from the fairly compact H II region or, in self-absorption, toward regions very nearby. For example, the CO($7 \rightarrow 6$) spectra (Jaffe et al. 1989) show no self-absorption at -3 km s^{-1} toward the [O I] peak position where we observed the absorption by the $+8$ km s^{-1} foreground cloud. It is quite conceivable that at this position most of the cold, molecular gas of the DR 21 cloud is behind the source of [O I] emission. In this case, of course, nothing can be said about the atomic oxygen abundance in that cloud. Clearly, similar observations of other clouds are needed for a final answer, but unfortunately they cannot be done until the advent of SOFIA.

5. CONCLUSIONS

1. We have presented the first observation of potential [O I] 63 μm absorption. The absorption, seen against the [O I] emission from the DR 21 outflow, would be due to a foreground molecular cloud at $v_{\mathrm{LSR}} \approx 8$ km s^{-1}.
2. The derived column density of cold, atomic oxygen is $\gtrsim 5 \times 10^{18}$ cm^{-2}, corresponding to a relative abundance of atomic oxygen of $[\mathrm{O}]/[\mathrm{H}] \gtrsim 6 \times 10^{-4}$. Therefore, most of the gas phase oxygen in this cloud would be in atomic form.
3. This result could answer the question of why all searches for molecular oxygen in the ISM have failed so far. Our finding could support chemistry models that predict a high fraction of the oxygen in molecular clouds to be in atomic form. However, this single observation may not be generalized because it cannot be precluded that this particular cloud is in an early phase of chemical evolution.

We would like to thank the crew of the Kuiper Airborne Observatory for their constant help in "getting the data," and the referee, F. Combes, for discussing the paper with us openly. This work was supported in part by NASA grant NAG2-208. N. G. was supported by a Feodor Lynen fellowship of the Alexander von Humboldt foundation.

REFERENCES

Anders, E., & Grevesse, N. 1989, Geochim. Cosmochim. Acta, 53, 197
Baluja, K. L., & Zeippen, C. J. 1988, J. Phys. B, 21, 1455
Bieging, J. H., Wilson, T. L., & Downes, D. 1982, A&AS, 49, 607
Cernicharo, J., Gonzáles-Alfonso, E., Alcoela, J., Bachiller, R., & John, D. 1994, ApJ, 432, L59
Combes, F., & Wiklind, T. 1995, A&A, 303, L61
Dickel, J. R., Dickel, H. R., & Wilson, W. J. 1978, ApJ, 223, 840
Dickel, J. R., Lubenow, A. F., Goss, W. M., Forster, J. R., & Rots, A. H. 1983, A&A, 120, 74
Fischer, J., Sanders, D. B., Simon, M., & Solomon, P. M. 1985, ApJ, 293, 508
Fuente, A., Cernicharo, J., García-Burillo, S., & Tejero, J. 1993, A&A, 275, 558
Garden, R. P., Hayashi, M., Gatley, I., Hasegawa, T., & Kaifu, N. 1991, ApJ, 374, 540
Gatley, I., Becklin, E. E., Werner, M. W., & Harper, D. A. 1978, ApJ, 220, 822
Goldsmith, P. F., Snell, R. L., Erickson, N. R., Dickman, R. L., Schloerb, F. P., & Irwine, W. M. 1985, ApJ, 289, 613
Gredel, R., Lepp, S., Dalgarno, A., & Herbst, E. 1989, ApJ, 347, 289
Greenberg, J. M. 1991, in Chemistry in Space, ed. J. M. Greenberg & V. Pironello (Dordrecht: Kluwer), 227
Herbst, E., & Leung, C. M. 1989, ApJS, 69, 271
Herrmann, F. 1993, Ph.D. thesis, Ludwig-Maximilians-Univ. München
Hildebrand, R. H., Loewenstein, R. F., Harper, D. A., Orton, G. S., Keene, J., & Whitcomb, S. E. 1985, Icarus, 64, 64
Jacq, T., Jewell, P. R., Henkel, C., Walmsley, C. M., & Baudry, A. 1988, A&A, 199, L5
Jacq, T., Walmsley, C. M., Henkel, C., Baudry, A., Mauersberger, R., & Jewell, P. R. 1990, A&A, 228, 447
Jaffe, D. T., Genzel, R., Harris, A. I., Lugten, J. B., Stacey, G. J., & Stutzki, J. 1989, ApJ, 344, 265

Knacke, R. F., & Larson, H. P. 1991, ApJ, 367, L162
Lane, A. P., Haas, M. R., Hollenbach, D. J., & Erickson, E. F. 1990, ApJ, 361, 132
Langer, W. D., & Graedel, T. E. 1989, ApJS, 69, 241
Liszt, H. S., & Vanden Bout, P. A. 1985, ApJ, 291, 178
Millar, T. J., Rawlings, J. M. C., Bennett, A., Brown, P. D., & Charnley, S. B. 1991, A&AS, 87, 585
Plambeck, R. L., & Wright, C. H. 1987, ApJ, 317, L101
Poglitsch, A., et al. 1991, Int. J. IR Millimeter Waves, 12, 895
Spitzer, L. 1978, Physical Processes in the Interstellar Medium (New York: Wiley)
Stacey, G. J., Beeman, J. W., Haller, E. E., Geis, N., Poglitsch, A., & Rumitz, M. 1992, Int. J. Infrared Millimeter Waves, 13, 1689
Sternberg, A., & Dalgarno, A. 1995, ApJS, 99, 565
Strong, A. W., Bloemen, J. B. G. M., Dame, T. M., Grenier, I. A., Hermsen, W., Lebrun, F., Nyman, L. A., Pollok, A. M. T., & Thaddeus, P. 1988, A&A, 207, 1
Tauber, J., Olofsson, G., Pilbratt, G., Nordh, L., & Frisk, U. 1996, A&A, in press
van Dishoeck, E. F., Blake, G. A., Draine, B. T., & Lunine, J. I. 1993, in Protostars and Planets III, ed. E. H. Levy & J. I. Lunine (Tucson: Univ. Arizona Press), 163
Zmuidzinas, J., Blake, G. A., Carlstrom, J., Keene, J., Miller, D., Schilke, P., & Ugras, N. G. 1995 in ASP Conf. Ser., Vol. 73, Proc. Airborne Astronomy Symp. on the Galactic Ecosystem: From Gas to Dust to Stars, ed. M. R. Haas, J. A. Davidson, & E. F. Erickson (San Francisco: ASP), 33